The EMBO Journal vol.13 no.11 pp.2677–2685, 1994

The decoding region of 16S RNA; a cross-linking study of the ribosomal A, P and E sites using tRNA derivatized at position 32 in the anticodon loop

Thomas Döring, Philip Mitchell[1], Monika Osswald, Dmitry Bochkariov[2] and Richard Brimacombe[3]

Max-Planck-Institut für Molekulare Genetik, Ihnestrasse 73, D-14195 Berlin, Germany
[1]Present address: EMBL, Postfach 1022.09, D-69117 Heidelberg, Germany
[2]Present address: Institute of Protein Research, Pushchino, 142292 Moscow Region, Russia
[3]Corresponding author

Communicated by C.Gualerzi

A photo-reactive diazirine derivative was attached to the 2-thiocytidine residue at position 32 of tRNA^{ArgI} from *Escherichia coli*. This modified tRNA was bound under suitable conditions to the A, P or E site of *E.coli* ribosomes. After photo-activation of the diazirine label, the sites of cross-linking to 16S rRNA were identified by our standard procedures. Each of the three tRNA binding sites showed a characteristic pattern of cross-linking. From tRNA at the A site, a major cross-link was observed to position 1378 of the 16S RNA, and a minor one to position 936. From the P site, there were major cross-links to positions 693 and to 957 and/or 966, as well as a minor cross-link to position 1338. The E site bound tRNA showed major cross-links to position 693 (identical to that from the P site) and to positions 1376/1378 (similar, but not identical, to the cross-link observed from the A site). Immunological analysis of the concomitantly cross-linked ribosomal proteins indicated that S7 was the major target of cross-linking from all three tRNA sites, with S11 as a minor product. The results are discussed in terms of the overall topography of the decoding region of the 30S ribosomal subunit.

Key words: cross-linking/photoreactive tRNA derivatives/ribonuclease H digestion/ribosomal A, P, E sites/16S RNA decoding region

Introduction

The question of the orientation of the tRNA molecules on the translating ribosome has been investigated in many laboratories by a variety of techniques. In recent years an increasingly widely used approach has been the 'site-directed cross-linking' method, whereby a suitably modified photo-reactive nucleotide is introduced at a specific position within the tRNA molecule, and, after binding to the ribosome and activation of the photo-label, the cross-linked ribosomal components are identified. So far, most of the studies using this approach (summarized by Wower *et al.*, 1993a) have concentrated on the identification of cross-linked ribosomal proteins. However, the proteins themselves are on average roughly half the size of a tRNA molecule or more, and as a result these data are only of limited value with regard to defining the detailed topography of the tRNA binding sites on the ribosome. A number of the corresponding studies involving the analysis of rRNA cross-linked to tRNA (also summarized by Wower *et al.*, 1993a) suffer from the same limitation, since the cross-links could only be localized within relatively long sections (30–100 nucleotides) of the rRNA molecules. In contrast, the number of investigations in which the analysis of the cross-linked sites has been pursued to nucleotide resolution is very small indeed. These sites include the cross-links from position 34 of the tRNA to nucleotide C-1400 of the *Escherichia coli* 16S RNA (Prince *et al.*, 1982), from position 76 of the tRNA to G-1945 of the 23S RNA (Wower *et al.*, 1989), and from position 47 of the tRNA to A-2309 of the 23S RNA (Mitchell *et al.*, 1993). In each case the tRNA was bound at the ribosomal P site, although similar cross-linking to C-1400 of the 16S RNA was observed using a rather long probe (23 Å) attached to position 34 of an A site bound tRNA (Ciesiolka *et al.*, 1985). The cross-links to 23S RNA from photo-affinity labelled amino acids in aminoacyl tRNA at the P or A sites (Steiner *et al.*, 1988; Mitchell *et al.*, 1993) are also relevant in this context. Detailed information at nucleotide resolution has been obtained from 'footprinting' studies of tRNA bound to the ribosomal A, P and E sites (e.g. Moazed and Noller, 1989, 1990), but the footprinting method has the disadvantage of being unable to distinguish between direct and allosteric effects, and is moreover unable to describe the orientations of the tRNA molecules at their respective binding sites.

What is clearly required at this stage is a systematic analysis at nucleotide resolution of cross-links to the rRNA from specific positions on tRNA molecules bound to each of the three ribosomal sites. In this context, the anticodon loop region of the tRNA is currently of particular interest to us, since we have recently identified a series of cross-link sites on the *E.coli* 16S RNA from mRNA analogues at several positions within or close to the coding triplets (Dontsova *et al.*, 1992; Rinke-Appel *et al.*, 1993); a combination of these latter results with a corresponding set of cross-linking data from the tRNA anticodon loop should lead to a much clearer picture of the topography of the decoding region of the 16S RNA as a whole.

In this paper we describe such a cross-linking analysis, using tRNA^{ArgI} from *E.coli*, which has a 2-thiocytidine residue at position 32 in the anticodon loop. In an earlier cross-linking study, Chen *et al.* (1985) attached a photo-reactive azido moiety to this residue and observed cross-linking to the 16S RNA, although they were not able to localize the cross-link site(s). Here, we have derivatized the thiocytidine in a similar manner with a newly developed diazirine reagent (cf. Bochkariov and Kogon, 1992), and we report the analysis of three distinct sets of cross-links to the 16S RNA, from the tRNA^{ArgI} bound to the A, P or E site.

A preliminary description of the set of P site cross-links has been published previously (Brimacombe *et al.*, 1993a,b).

Results

The synthesis of the diazirine cross-linking reagent, 3-[3-(bromoacetylamino)phenyl]-3-(trifluoromethyl)diazirine (BAPTD), is described in Materials and methods (and see Figure 6 below). The reagent is able to react with thionucleotides via the bromoacetylamino group (cf. Hixson and Hixson, 1975), and the diazirine moiety can be activated by irradiation at wavelengths above 300 nm (cf. Bochkariov and Kogon, 1992). The BAPTD was coupled to ^{32}P-labelled tRNA^{ArgI} from *E.coli*, and the derivatized tRNA (either charged or uncharged) was incubated with ribosomes under a variety of conditions specific for binding to the A, P or E sites. Either 70S tight couples or 70S complexes reconstituted from 30S and 50S subunits were used and the binding was carried out in the presence of appropriate mRNA analogues, prepared by T7 transcription from synthetic DNA templates. The sequences of these mRNA molecules are listed in Figure 1.

For A site binding, mRNA 1 (Figure 1) was used. In this case, tRNA^{fMet} was bound first via the AUG triplet, and then BAPTD-derivatized Arg-tRNA^{ArgI} was added so as to bind to the adjacent cognate CGU codon at the A site. [CGU has been shown to be the most effective codon for binding modified tRNA^{ArgI} (Kruse *et al.*, 1978).] Control incubations were done either in the absence of mRNA, or using mRNA 4 which has a non-cognate A site codon. P site binding was carried out with BAPTD-tRNA^{ArgI} either in the absence of mRNA, or using mRNA 2, which carries an arginine CGU triplet, but no AUG. The same mRNA (No. 2) was also used for binding to the E site. In this case tRNA^{Phe} was first bound via the UUC triplet, with subsequent binding of BAPTD-tRNA^{ArgI} to the cognate CGU codon now at the E site. In other E site binding experiments, mRNAs 3 or 4 were used, and tRNA^{fMet} was first bound to the AUG triplet, so as to expose either a cognate CGU triplet (mRNA 3) or a non-cognate AAG (mRNA 4) at the E site; this is of course a 'non-physiological' situation, but is nevertheless of experimental interest. Details of the individual binding reactions are given in Materials and methods.

Each BAPTD-tRNA−mRNA−ribosome complex was irradiated with UV light (350 nm), and the cross-linked products were separated by a series of sucrose gradients (Stade *et al.*, 1989). The first sucrose gradient (at high magnesium) serves to separate the 70S complex from unbound tRNA and mRNA, and the second (at low magnesium) separates the 30S and 50S subunits, as well as dissociating the bound mRNA and non-cross-linked ^{32}P-labelled tRNA. Cross-linking was only observed to the 30S subunit in these experiments, and in a final sucrose gradient (in the presence of SDS) the 30S subunits were dissociated into a 16S RNA and a protein fraction, each containing the respective components cross-linked to tRNA. [These data are not shown, but precisely analogous gradient profiles can be seen in Stade *et al.* (1989) or Rinke-Appel *et al.* (1991).]

The carbene radical generated by photo-activation of a diazirine is extremely short-lived and highly reactive (Brunner *et al.*, 1980). This has the advantage that the carbene takes an instantaneous 'snapshot' of its environment in the cross-linking process, rather than seeking a preferred reaction partner as is the case with longer-lived radicals. On the other hand, the high reactivity unavoidably also leads to a high level of reaction with the solvent, so that the yields of cross-linking to the ribosomal components (calculated from the radioactivity in the SDS−sucrose gradients) are correspondingly low, usually of the order of 1−2% to the rRNA, and 4−6% to the ribosomal proteins (cf. Bochkariov and Kogon, 1992). In view of the low percentage of reaction with the 16S RNA, every cross-link analysis of the RNA moiety in the various samples or controls was pursued to the level of identification of the cross-linked regions in the 16S sequence; only at this level could the specificities and quantitative distribution of the individual cross-links be

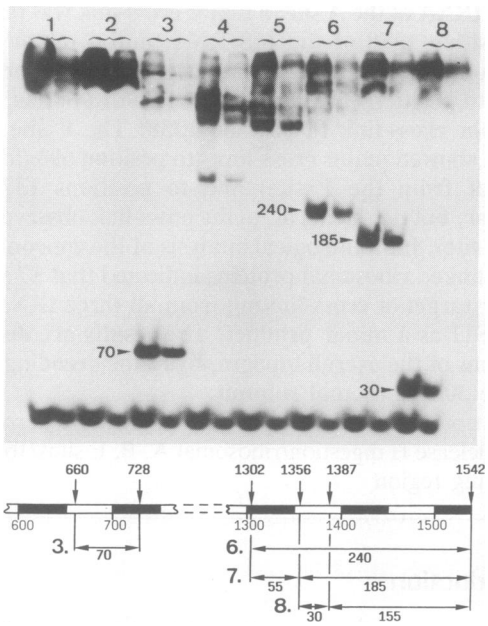

Fig. 2. Ribonuclease H digests of a cross-linked E site BAPTD-tRNA^{ArgI}−16S RNA complex, containing ^{32}P-labelled tRNA, on a 5% polyacrylamide gel (Rinke-Appel *et al.*, 1991). In each pair of slots the right-hand sample is from a control experiment where the tRNA^{ArgI} had been irradiated prior to derivatization with BAPTD (see text). The ribonuclease H digestions were performed in the presence of pairs of oligodeoxynucleotides (10- or 17-mers) centred on 16S positions 332/489 (lanes 1), 489/660 (lanes 2), 660/728 (lanes 3), 728/918 (lanes 4), 918/977 (lanes 5), 977/1302 (lanes 6), 1302/1356 (lanes 7) and 1356/1387 (lanes 8). The approximate lengths of the 16S RNA fragments in each band are indicated, and the locations of these fragments within the 16S RNA are shown schematically in the lower part of the figure, arranged according to lane number. (The fast-moving band in each gel slot corresponds to free tRNA; see text.)

E P A

1. . . . GGGAGAAAAGA GAA AUG CGU AAA AAC AAA AAC AAA AAC

2. . . . GGGAGAAAAGA AAG CGU UUC AAA GGG AAC AAA AAC AAA AAC

3. . . . GGGAGAAAAGA CGU AUG GAA AAA AAC AAA AAC AAA AAC

4. .GGGAGAAGGAGAAAAG AAG AUG UUC AAA AGA AAA

Fig. 1. The synthetic mRNA sequences used for binding to the A, P or E sites. Codons for tRNA^{ArgI} (CGU), tRNA^{fMet} (AUG) or tRNA^{Phe} (UUC) are in heavy type, and Shine−Dalgarno sequences are underlined. (Note: mRNA 4 was originally designed for a different experimental programme.)

unambiguously compared. Determination of the cross-linked regions in the 16S RNA was done by the ribonuclease H method (Rinke-Appel *et al.*, 1991), whereby the [^{32}P]tRNA–16S RNA complex is digested with ribonuclease H in the presence of pairs of oligodeoxynucleotides complementary to selected sequences of the 16S RNA; a typical example of such an analysis, together with one particular set of controls, is illustrated in Figure 2. (See below for descriptions of other types of control experiment.)

In each pair of slots in Figure 2 the left-hand sample is from 70S tight couple ribosomes carrying ^{32}P-labelled derivatized tRNA^{ArgI} at the E site in the presence of mRNA 3 (Figure 1) as described above (a precisely similar gel pattern was observed with mRNA 2). The right-hand control sample in each pair of slots is the same, but using tRNA^{ArgI} that had been irradiated at 350 nm prior to modification with the diazirine reagent; tRNA^{ArgI} contains a 4-thiouridine residue at position 8 in addition to the thiocytidine at position 32 (Sprinzl *et al.*, 1989), and thiouridine at this position in tRNA is quantitatively cross-linked to a cytidine residue at position 13 by irradiation at 350 nm (Ofengand *et al.*, 1974). We confirmed (data not shown) that this latter observation holds true in the case of tRNA^{ArgI} by making a kinetic analysis of the photo-reaction, exactly as described by Ofengand *et al.* (1974). In the pre-irradiated tRNA^{ArgI}, the thiouridine residue is therefore not available for reaction with the BAPTD, and any observed cross-linking must arise from the derivatized thiocytidine at position 32 (Chen *et al.*, 1985). Figure 2 shows that the cross-linking pattern is indeed identical in each pair of slots (the band intensities from the pre-irradiated control sample are slightly weaker, because the initial binding of the pre-irradiated tRNA to the 70S ribosomes was somewhat lower). Two distinct cross-linked regions can be seen in these E site samples; the first lies between positions 660 and 728 of the 16S RNA (lanes 3, Figure 2), and the second is progressively localized by the digestions in lanes 6, 7 and 8 to the region between positions 1356 and 1387. (The faint bands in lanes 4 do not correspond to an expected digestion product, and therefore represent a spurious cut by the ribonuclease H; see below for further discussion of this point.)

Figure 2 shows that significant amounts of free tRNA are present in the ribonuclease H digests, as evidenced by the fast-moving band in each gel slot. This effect is in part due to tRNA remaining non-covalently associated with the 16S RNA even after the sucrose gradient separations, but some tRNA is also released from the cross-linked complexes during the ribonuclease incubation at 55°C; the latter contribution could be minimized by reducing the time of the ribonuclease H treatment (see Materials and methods). 2-Thiocytidine derivatives are known to be susceptible to nucleophilic attack (Kröger *et al.*, 1976), but no differences in either the overall cross-linking yields or the amount of tRNA released were observed when the entire cross-linking experiment and analysis were carried out in the absence of primary amine-containing buffers, and with potassium ions in place of ammonium ions. Additional control experiments similar to that of Figure 2 showed that the cross-linking from BAPTD-tRNA^{ArgI} was abolished if the tRNA was treated with iodoacetamide, which reacts specifically with the thiocytidine residue (Kruse *et al.*, 1978), prior to derivatization with BAPTD. Furthermore, as we have already reported (Brimacombe *et al.*, 1993a), no cross-linking was observed when tRNA^{Phe}, which carries the 4-thiouridine residue at position 8, but has no thiocytidine, was used in place of tRNA^{ArgI}; these latter controls were made with BAPTD-treated tRNA^{Phe} using mRNA 2 (Figure 1) for P site binding of the tRNA^{Phe} or mRNA 4 for A site binding of Phe-tRNA^{Phe}. The cross-linking with tRNA^{ArgI} was also abolished if the BAPTD-tRNA–mRNA–ribosome complexes were not subjected to UV irradiation, or if this irradiation step was included but the BAPTD derivatization omitted. Taken together, these controls indicate clearly that the observed cross-linking (cf. Figure 2) was BAPTD dependent and specific for position 32 of the tRNA^{ArgI}.

The ribonuclease H technique was used in a similar manner to compare the patterns of cross-linking to 16S RNA from tRNA^{ArgI} at the A, P or E sites. Scans of the complete 16S molecule (such as the experiment of Figure 2) had revealed four distinct regions containing cross-links, and the appropriate ribonuclease H digestions for the three tRNA sites are shown in Figure 3. The gels in Figure 3 were derived from a single experiment, starting with equal amounts of ribosomes in each of the three (A, P and E site) analyses (see Materials and methods). The A site analysis was done in this case with BAPTD-derivatized Arg-tRNA^{ArgI} bound to 70S tight couples in the presence of tRNA^{fMet} and mRNA 1 (Figure 1), the P site analysis with BAPTD-tRNA^{ArgI} bound to 70S reconstituted complexes in the absence of mRNA, and the E site analysis with BAPTD-tRNA^{ArgI} bound to 70S tight couples in the presence of tRNA^{fMet} and mRNA 3. (The effects of the various different conditions used for binding to the A, P and E sites are discussed below.) In Figure 3a, the ribonuclease H digestions were done with oligodeoxynucleotides centred on positions 660 and 728 of the 16S RNA, and it can be seen that a corresponding radioactive 70-nucleotide 16S RNA fragment cross-linked to [^{32}P]tRNA was released from both the P and E site samples, but not from the A site sample.

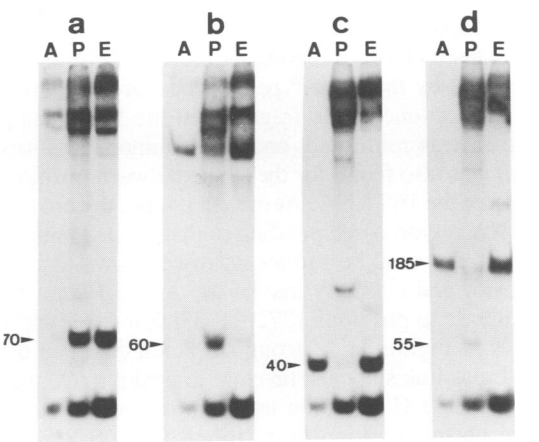

Fig. 3. Ribonuclease H digests of cross-linked A, P or E site BAPTD-tRNA^{ArgI}–16S RNA complexes, containing ^{32}P-labelled tRNA, as in Figure 2. In (**a**) the digestions were done in the presence of pairs of oligodeoxynucleotides centred on 16S positions 660/728 (releasing a ~70-nucleotide 16S RNA fragment), in (**b**) positions 918/976 (a 60-nucleotide fragment), in (**c**) positions 1356/1397 (a 40-nucleotide fragment), and in (**d**) positions 1302/1356 (releasing a 55-nucleotide fragment between these two positions, and a 185-nucleotide fragment between position 1356 and the 3′-end of the molecule).

In Figure 3b, with oligodeoxynucleotides centred on positions 918 and 976, the corresponding 60-nucleotide fragment was only observed in the P site sample, whereas in Figure 3c, covering positions 1356–1397, a 40-nucleotide fragment appears in the A and E site samples. Thus, each tRNA site gives a characteristic pattern of cross-linking, with the P site showing strong cross-links in Figure 3a and b, the E site in Figure 3a and c, and the A site in Figure 3c only. Notably, the intensity of the A site cross-linked band in Figure 3c is comparable with that of the major P and E site bands, although the overall level of cross-linking (as evidenced by the total amount of radioactivity in each gel slot) is clearly lower in the A site samples. At this point it should be noted that, in addition to the major cross-linked bands, faint bands can be seen at the expected fragment positions in all the gel slots in Figure 3a, b and c (e.g. from the A and E site samples in Figure 3b). This clearly reflects low levels of cross-contamination between the A, P and E sites, and emphasizes the importance of carrying out this type of experiment with all three tRNA binding sites in parallel (see also Discussion).

In Figure 3d, the oligodeoxynucleotides used in the ribonuclease H digestion were centred on positions 1302 and 1356 of the 16S RNA. Here, a weak 55-nucleotide fragment is visible in the P site sample, but not in either the A or the E site samples, both of which show instead a strong 185-nucleotide cross-linked fragment; the latter represents the region of 16S RNA 3′ with respect to the cutting site at position ~1356, and thus these A and E site bands correspond to the same cross-link as that of Figure 3c (cf. slots 7 and 8 of Figure 2). A small number of weak spurious ribonuclease H cuts can be seen in Figure 3 (cf. slot 4 in Figure 2, above); for example the P site sample in Figure 3c shows a band of ~150 nucleotides, which could be interpreted as a cross-link downstream from the cutting site at position 1397 of the 16S RNA. However, this was not substantiated by other ribonuclease H digestions covering the 3′-region, and similar spurious cuts could always be identified as such by varying the oligodeoxynucleotide pairs used in the digestion mixtures. (The spurious cuts arise from statistical partial complementarities of the oligodeoxynucleotides with other regions of the 16S RNA sequence.) In contrast, by the same type of procedure, the cross-link within the 55-nucleotide fragment in the P site sample of Figure 3d was confirmed, and a new minor cross-link (not shown) was also found for the A site between positions 925 and 948 of the 16S RNA. At the same time, the cross-linked 16S RNA region corresponding to that of the P site sample in Figure 3b could be further narrowed down to positions 948–976, and similarly that of the A and E site samples in Figure 3c to positions 1372–1385. For the P and E site samples in Figure 3a, a strong suspicion emerged that the actual cross-link site must lie close to position 690, because a ribonuclease H digestion using an oligodeoxynucleotide centred on this position failed to cut the 16S RNA in the cross-linked samples.

The pattern of cross-linking observed from the A site was the same, regardless of whether 70S tight couple ribosomes or reconstituted complexes were used, and this A site cross-linking was reduced to 'background' levels (cf. Figure 3) in the absence of mRNA, or if an mRNA with a non-cognate A site codon (mRNA 4, Figure 1) was used in place of mRNA 1. The corresponding E site patterns were essentially invariable under all conditions tested, either with 70S tight couples or reconstituted complexes, with an AUG codon (plus $tRNA^{fMet}$) or a UUC codon (plus $tRNA^{Phe}$) at the P site, and with or without a CGU codon cognate to $tRNA^{ArgI}$ at the E site. [It is known (Gnirke *et al.*, 1989; Schilling-Bartetzko *et al.*, 1992) that the importance of codon–anticodon interaction at the E-site is less pronounced at the magnesium concentrations of 15–20 mM used in our study.] In contrast, the P site cross-linking was rather more sensitive to the precise conditions used; the levels of cross-linking were lower with 70S tight couples [particularly in the case of the 948–976 region (cf. Figure 3b)] than with reconstituted complexes, and were higher in the absence of mRNA. Furthermore, with 70S tight couples, significant P site cross-linking to the 1372–1397 region of the 16S RNA was observed (cf. Brimacombe *et al.*, 1993b; see below for further discussion), whereas this was not the case with the reconstituted complexes (Figure 3c). Additional binding of a second tRNA to either the A or the E site did not have any significant influence on the pattern of P site cross-linking (data not shown).

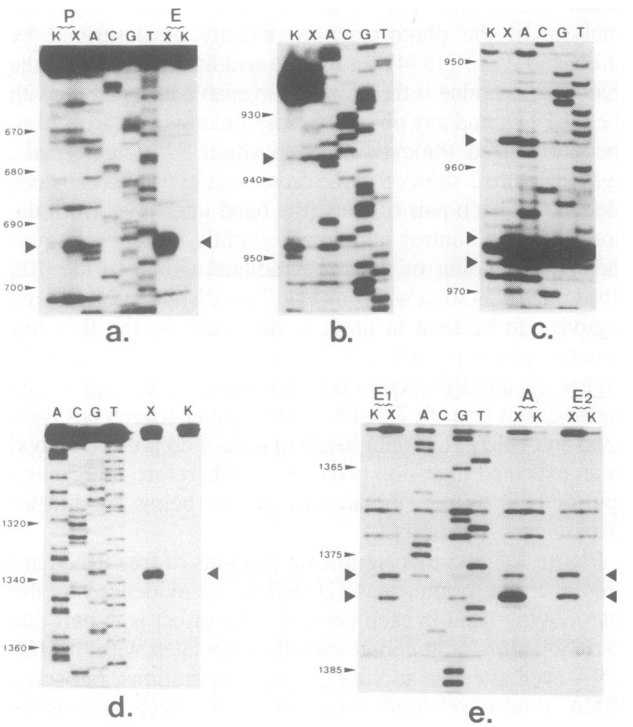

Fig. 4. Primer extension analyses (Moazed and Noller, 1986) of the individual cross-linked complexes. In each case lane X is the cross-linked sample, isolated as a complex containing a 100–200 nucleotide fragment of 16S RNA by ribonuclease H digestion as in Figure 2 or 3, and lane K is the corresponding free 16S RNA fragment, isolated from the same gel lane. A, C, G and T are dideoxy sequencing lanes. In each part of Figure 3 appropriate regions of the (10%) sequencing gels are shown, with the stop signals corresponding to the cross-link sites being indicated by the solid triangles. (**a**) Samples derived from P or E site bound tRNA, as indicated. The primer for the reverse transcriptase reaction was complementary to 16S positions 760–776. (**b**) An A site sample, with primer complementary to positions 996–1012. (**c**) P site sample, with primer as in (b). (**d**) P site sample, with primer complementary to positions 1491–1507. (**e**) A and E site samples, as indicated, with primer complementary to positions 1412–1427. (Sample E_1 is derived from an experiment with a non-cognate mRNA codon at the E site, E_2 with a cognate codon; see text.)

Further localization of the cross-link sites within the 16S RNA regions deduced from the ribonuclease H digestions was done by the primer extension method (Moazed *et al.*, 1986). For this purpose, suitable fragments containing ~100–200 nucleotides of the 16S RNA encompassing each cross-link site were excised from the ^{32}P-labelled cross-linked complexes, again using ribonuclease H. These fragments were separated by gel electrophoresis as in Figures 2 and 3, and corresponding control fragments of non-cross-linked 16S RNA (located by their UV absorption) were isolated from the same gel lanes. The reverse transcriptase analyses were made using oligodeoxynucleotide primers complementary to sites downstream from the cross-linked regions in the 16S RNA, and examples of the gels obtained are illustrated in Figure 4.

Figure 4a shows the data for the P and E site cross-links between positions 660 and 728 of the 16S RNA (Figure 3a). In both cases, a strong stop signal can be seen in the cross-linked samples at nucleotide A-694, consistent with the prediction (see above) that this cross-link must lie close to position 690. Figure 4b shows the minor A site cross-link mentioned above between positions 925 and 948, where the stop signal is at nucleotide A-937. In Figure 4c, corresponding to the P site cross-link between positions 918 and 976 (Figure 3b), stop signals are visible both at nucleotide A-958 and in the region of the methylated bases at nearby nucleotides G-966 and C-967 (see also Brimacombe *et al.*, 1993a); these sites are consistent with the ribonuclease H data noted above, in which the 16S RNA region containing this cross-link was further localized to positions 948–976. Figure 4d shows the minor P site cross-link between positions 1302 and 1356 of the 16S RNA (Figure 3d), and a clear stop signal at nucleotide A-1339 can be seen. The final example, Figure 4e, gives typical data for the A and E site cross-links between positions 1356 and 1397 (Figure 3c), further localized as already mentioned to positions 1372–1385. Two E site samples are shown, the first (E_1) from an experiment with a non-cognate codon in the mRNA at the E site, and the second (E_2) with a cognate codon. In both cases two stop signals of approximately equal intensity are visible in the cross-linked samples, at nucleotides A-1377 and G-1379. However, in the A site sample, although the same two signals are present, that at G-1379 is considerably stronger. This effect was very reproducible, and in some experiments the signal at A-1377 was even entirely absent from the A site sample, whereas in the E site samples the stop at A-1377 tended to be the stronger of the two. The A site and E site cross-links at this position are thus subtly distinguishable from one another. All of these cross-link data are summarized in Table I, making the usual assumption that the actual sites of cross-linking are one base upstream from the observed stop signals the reverse transcriptase gels (Figure 4).

It should be noted here that additional apparent cross-link sites are often observed on the reverse transcriptase gels outside the regions defined by the ribonuclease H digestion data. An example can be seen at nucleotide A-1360 in Figure 4e. Conversely, stop signals are sometimes seen in the control lanes (e.g. at nucleotide U-950 in Figure 4b) where no signal is visible in the corresponding cross-linked sample. This type of reverse transcriptase artefact is discussed further below.

In all of the experiments described here, the cross-linking to 16S RNA was accompanied by a concomitant cross-linking to ribosomal protein. The 30S protein fractions from the SDS–sucrose gradients used to separate the cross-linked 16S RNA were routinely analysed, by the immobilized antibody–agarose method (Gulle *et al.*, 1988; Stade *et al.*, 1989). However, in contrast to the highly differentiated pattern of cross-linking observed with the 16S RNA (Table I), the A, P and E site tRNA samples all gave the same pattern of cross-linking to ribosomal protein. The major target of cross-linking was S7, with S11 showing a minor contribution, and only in the case of cross-links from P site tRNA bound to reconstituted 70S complexes was any difference observed; here S13 was found in place of S11 (data not shown).

Table I. Specificity of cross-linking to the A, P and E sites

Position in 16S RNA	tRNA binding site		
	A	P	E
693	–	++	++
936	+	–	–
957/966	–	++	–
1338	–	+	–
1376/1378	–	–[a]	++
1378	++	–	–

The intensity of each cross-link is denoted by ++ (major), or + (minor). The symbol '–' means that the cross-link concerned was either absent or drastically reduced in relation to the corresponding cross-link from one of the other two tRNA sites (cf. Figure 3).
[a]Minor cross-linking to this site was observed when 70S tight couples rather than reconstituted complexes were used (see text).

Discussion

The locations of the A, P and E site cross-links from position 32 of tRNA^{ArgI} (Table I) in the corresponding regions of the secondary structure of the 16S RNA are illustrated in Figure 5. The figure also shows other data relevant to the interaction between tRNA and 16S RNA, including the cross-link from position 34 of P site bound tRNA to nucleotide C-1400 (Prince *et al.*, 1982), cross-links from mRNA to 16S RNA at positions close to or within the decoding region (Rinke-Appel *et al.*, 1993; J.Rinke-Appel, N.Jünke, R.Brimacombe, I.Lavrik, S.Dokudovskaya, O.Dontsova and A.Bogdanov, in preparation), sites of footprinting for A or P site bound tRNA (Moazed and Noller, 1990), and sites of cross-linking to ribosomal proteins S7, S11, S13 and S19 (Brimacombe *et al.*, 1988). Cross-links from specific positions within the anticodon stem–loop region of tRNA have been reported to S7 with P or A site bound tRNA (Podkowinski and Gornicki, 1989; Sylvers *et al.*, 1992), to S13 and S19 with P site bound tRNA (Wower *et al.*, 1990), and to S11 with E site bound tRNA (Wower *et al.*, 1993b). Our own data provide further evidence for the involvement of S7, S11 and S13, but, as already discussed above, the cross-links to ribosomal proteins are less differentiated than those to the 16S RNA and are of limited interest with regard to a study of the detailed topography of the ribosomal decoding region.

Each of the tRNA binding sites shows a distinctive pattern of cross-linking to 16S RNA (Table I and Figure 5), but the patterns do partially overlap, with the P and E sites both

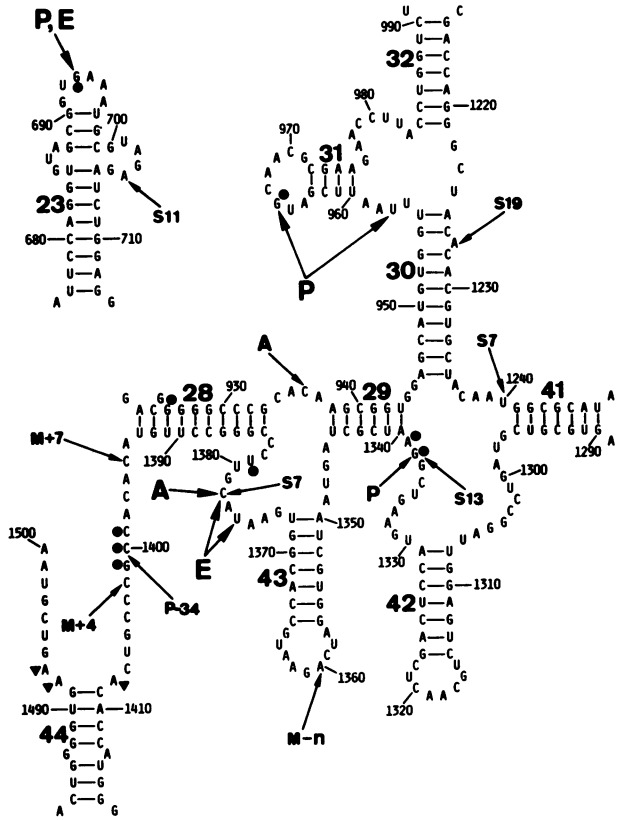

Fig. 5. Locations of the cross-link sites (Table I) in the corresponding regions of the secondary structure of 16S RNA. The helices are numbered as in Brimacombe (1991). The A, P and E site cross-links are denoted by large letters (major cross-links) or smaller letters (minor cross-links) as appropriate. 'M+4' and 'M+7' indicate sites of cross-linking to mRNA at the +4 and +7 positions, respectively (Rinke-Appel *et al.*, 1993), and 'M-n' a site of cross-linking to mRNA in the spacer region between the Shine–Dalgarno sequence and the AUG start codon (J.Rinke-Appel *et al.*, in preparation). 'P-34' indicates the site of cross-linking to position 34 of P site bound tRNA (Prince *et al.*, 1982). Solid triangles and circles denote sites of footprinting from A or P site bound tRNA, respectively (Moazed and Noller, 1990). Sites of cross-linking to ribosomal proteins S7, S11, S13 and S19 (Brimacombe *et al.*, 1988) are also included.

giving a cross-link at position 693, and the A and E sites a cross-link at position 1378. In such a situation it is particularly important to make parallel analyses of the cross-links from all three sites, as we have done here, in order to avoid assigning individual cross-links to the wrong tRNA binding sites. The usual type of functional test, such as a puromycin reaction, is not sensitive enough to make unequivocal tRNA site assignments for the various cross-links in our experiments, because the intensities of the cross-links are very low and vary over a relatively wide range. This point is illustrated by the 'P site' cross-links to regions 1356–1397 and 1302–1356 of the 16S RNA (Figure 3c and d, respectively), where in each case weak bands can be seen in the P site lanes (at the 40-nucleotide position in Figure 3c and in the 55-nucleotide position in Figure 3d). However, in comparison with the corresponding A and E site patterns in Figure 3, it is clear that the apparent P site cross-link in the 1356–1397 region (Figure 3c) is a cross-contamination from one of the other two sites, whereas that in the 1302–1356 region (Figure 3d) is indeed specific for the P site. On the other hand, as already noted above, significant P site cross-linking to the 1356–1397 region was observed when 70S tight couples were used in place of reconstituted complexes, and accordingly in our previous preliminary P site analysis (Brimacombe *et al.*, 1993b) we had tentatively assigned the cross-links at both positions 1378 and 1338 to the P site.

In view of the continuing discussion in the literature concerning the properties of the tRNA binding sites, in particular those of the E site (Gnirke *et al.*, 1989; Wower *et al.*, 1993b), we used a number of different conditions for tRNA binding (see Materials and methods). In fact, however, the only significant variation to emerge from the comparison of different conditions was the question of the P site cross-linking to nucleotide 1378, as just mentioned. At this stage it is not possible to distinguish whether the P site cross-linking to this position with 70S tight couples represents an A or E site contamination, or whether the P site itself is subtly different in the two types of 70S particle. We had expected to obtain further confirmation of the site specificity of the cross-links by making translocations with EF-G prior to photo-activation of the diazirine label; this method had provided valuable information in our site-directed cross-linking experiments with mRNA analogues (Dontsova *et al.*, 1992; Rinke-Appel *et al.*, 1993), but here repeated attempts to translocate BAPTD-derivatized Arg-tRNA^{Arg}I from the A to the P site were unsuccessful, suggesting that the derivatization of position 32 of the tRNA anticodon loop may block the translocation reaction.

A further technical question of more general significance is our observation of artefacts in the primer extension analyses, whereby apparent additional cross-link sites (or anomalous stop signals in the control samples) were seen on the reverse transcriptase gels, outside the regions that had been unambiguously defined by a series of ribonuclease H digestions using different pairs of oligodeoxynucleotides. These effects can be explained by the fact that in a cross-linking analysis (as opposed for example to a footprinting assay) the ligand under study, in this case the tRNA, remains covalently attached to the rRNA during the primer extension process. During the annealing reaction with the primer, the relatively large tRNA molecule can form fortuitous secondary and tertiary structures with the rRNA fragment, and these artefactual structures can give rise to different sets of stop or pause signals in the corresponding cross-linked or control sample lanes, in a manner which is reproducible but dependent on the length of the particular RNA fragment used for the primer extension assay. This underscores the importance of first using the ribonuclease H method for localization of the cross-link sites to within as small a region of the rRNA as possible (Tate *et al.*, 1990; Dontsova *et al.*, 1992; Rinke-Appel *et al.*, 1991, 1993). By the same argument, it follows that in cases where two sites are observed close together within such a region (for example the P site cross-links at positions 957 and 966, Table I), it cannot be excluded that one of the sites is a reverse transcriptase artefact. It also follows that similar cross-linking studies in the literature, which rely exclusively on the primer extension method (e.g. Bhangu and Wollenzien, 1992; Nolan *et al.*, 1993), should be regarded with caution.

BAPTD is a relatively short cross-linking reagent (8.5 Å), and therefore the cross-links observed to 16S RNA (Table I) must lie within approximately a one-nucleotide distance (in terms of the phosphate–phosphate backbone) from position

32 of the $tRNA^{ArgI}$. Taken together with the other data (Figure 5), the cross-links provide a new insight into the topography of the decoding region of the 16S RNA and in particular indicate that the area surrounding helices 28, 29, 43 and 44 must be folded in an extremely convoluted fashion involving all three tRNA binding sites. Thus, beginning at the lower left-hand corner of Figure 5, there are A site tRNA footprint positions (Moazed and Noller, 1990) located at the upper end of helix 44. Nearby, at nucleotide 1402, there is a cross-link to position +4 within the A site codon of mRNA (Rinke-Appel *et al.*, 1993), and immediately adjacent are the P site tRNA footprint positions (Moazed and Noller, 1990) and the cross-link from position 34 of P site tRNA to nucleotide C-1400 (Prince *et al.*, 1982). Next, at nucleotide 1395 is the cross-link to position +7 of the mRNA, just downstream of the A site codon (Dontsova *et al.*, 1992), which is in turn close to a P site footprint at nucleotide 926 in helix 28. The single-stranded 'ring' connecting helices 28, 29 and 43 contains both of the $tRNA^{ArgI}$ A site cross-links (Table I), as well as the E site cross-link at nucleotides 1376–1378 and another P site footprint at nucleotide 1381 (Moazed and Noller, 1990). The P site cross-link at nucleotide 1338 (Table I) adjacent to helix 29 coincides with a P site footprint at the same position. In the loop-end of helix 43 there is a cross-link to the spacer region of mRNA between the Shine–Dalgarno sequence and the AUG codon (J.Rinke-Appel *et al.*, in preparation), which is thus within or upstream of the E site. A similar cross-link from the upstream region of mRNA to the extreme 3′-terminal region of 16S RNA (Stade *et al.*, 1989), and the cross-link from position 37 of E site bound tRNA, also to the 3′-terminal region of 16S RNA (Wower *et al.*, 1993b), are also relevant in this context.

Particularly intriguing is the finding of coincident major cross-links to nucleotide 1378 from both the A site and the E site, but at most only minor cross-linking to this position from the P site (Table I). This implies that either the anticodon loop region of the E site tRNA must be oriented back towards the A site, or that the single-stranded sequence containing these cross-link sites (nucleotides 1373–1383) must be flexible and able to move from the A to the E site. Whichever possibility is correct, it seems likely that this finding is related to the 'allosteric linkage' (Gnirke *et al.*, 1989) between the A and E sites. A further striking feature of the data is the degree of coincidence between the cross-link positions and P-site footprints, a phenomenon which has also been noted in the 23S RNA, with regard to cross-links from the aminoacyl moiety of tRNA (Steiner *et al.*, 1988; Mitchell *et al.*, 1993) and footprints from its 3′-terminus (Moazed and Noller, 1989). In addition to those cases just discussed, the P site cross-link at nucleotide 966 in helix 31 and the P and E site cross-links at nucleotide 693 in helix 23 (Figure 5) are identical with P site footprint positions (Moazed and Noller, 1990); from the cross-link data, it can be concluded that the loop-ends of these two helices (23 and 31) are indeed directly involved in the decoding region. From similar cross-linking studies with mRNA, helices 18 and 34 (Dontsova *et al.*, 1992) and now helix 22 (J.Rinke-Appel *et al.*, in preparation) are also part of the same neighbourhood. All of these results place strong constraints on the three-dimensional folding of the 16S RNA in the decoding area.

Materials and methods

Synthesis of BAPTD

The reaction scheme is shown in Figure 6. The starting material, α,α,α-trifluoroacetophenone (compound I, Figure 6, from Fluka) was converted to the *m*-nitro derivative (II) according to Stewart and Van der Linden (1960), and then reduced to the corresponding amine (III) as described by Klabunde and Burton (1970). 3-[-*m*-(formylamino)phenyl]-3-(trifluoromethyl) diaziridine (VII) was synthesized from III as described by Brunner and Semenza (1981), and oxidized to the corresponding diazirine (VIII) as described by Dolder *et al.* (1990).

The diazirine VIII (300 mg, 1.3 mmol) was dissolved in methanol (5 ml). Concentrated HCl (2.5 ml) was then added and the mixture incubated for 30 min at room temperature. The mixture was extracted twice with ether and the aqueous phase adjusted to pH 11 by addition of 20% KOH. The aryl amine (IX) was extracted from this solution with two portions of ether, and the combined organic phase was washed with water, dried over Na_2SO_4 and evaporated. 3-(*m*-aminophenyl)-3-(trifluoromethyl)-diazirine (IX) is a slowly crystallizing orange oil. The yield was 190 mg (0.95 mmol, 73%), and the product was used for the following step without further purification.

The aryl amine IX (190 mg) was dissolved in dry dioxan (5 ml). A solution of bromoacetyl bromide (483 mg, 1.5 mmol) in dry dioxan (5 ml) was then added. After 1 min at room temperature a precipitate appeared. Next, a solution of triethylamine (101 mg, 1 mmol) in dry dioxan (2.5 ml) was added in a single aliquot to the well-stirred reaction mixture; the precipitate already formed dissolved, and a fresh precipitate appeared after several seconds. The reaction proceeds very rapidly, and no additional incubation was necessary. The reaction mixture was diluted with water (100 ml) and extracted twice with ether. The combined organic phase was washed with 5% $NaHCO_3$, then with water, and was dried over Na_2SO_4 and evaporated. The residue was dissolved in ether (1.5 ml) and hexane was added (30 ml). The mixture was cooled to −20°C for 3 h, and the final product, BAPTD (X, Figure 6), crystallized from this solution as long white needles. The crystals were filtered off, washed with cold hexane and dried. The product (220 mg, 0.68 mmol, 72%) does not need any further purification. The structure of the BAPTD was proved by recording its NMR and mass spectra. The substance gave a melting point of 76–77°C and showed the expected C, H and N values upon elemental analysis. The UV spectrum showed maxima at 249 nm (E = 12 250) and 355 nm (E = 399), the latter peak, due to the diazirine moiety, disappearing completely upon irradiation with UV light at wavelengths >300 nm.

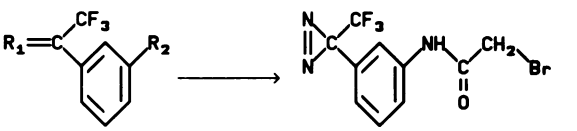

	R_1	R_2
I	=O	–H
II	=O	$–NO_2$
III	=O	$–NH_2$
IV	=O	–NHCHO
V	=NOH	–NHCHO
VI	=NOTos	–NHCHO
VII		–NHCHO
VIII		–NHCHO
IX		$–NH_2$
X		$–NH–C(=O)–CH_2Br$

Fig. 6. Reaction scheme for the synthesis of BAPTD (see Materials and methods). The distance between the reactive carbon atoms is 8.5 Å.

Derivatization of tRNA^{Arg}I with BAPTD and charging with arginine

tRNA^{Arg}I (Subriden RNA, USA) was labelled with ^{32}P at its 5′-end (specific activity ~40 000 c.p.m./pmol) as described by Gnirke *et al.* (1989) and then treated with BAPTD in dimethyl sulfoxide under the conditions of Bochkariov and Kogon (1992). This uncharged derivatized tRNA was used for P or E site binding experiments. For A site binding, the ^{32}P-labelled tRNA was charged with arginine before derivatization with BAPTD, according to Rheinberger *et al.* (1988); after the charging reaction the Arg-tRNA^{Arg}I was separated from low molecular weight contaminants by gel filtration on a NICK column (Pharmacia, 0.9×2.0 cm), using water as eluant. The level of charging with arginine was ~70%, as determined in parallel experiments with ^{3}H-labelled arginine and unlabelled tRNA^{Arg}I. In control experiments (at all three tRNA sites) the tRNA was either irradiated at 350 nm (which leads to a quantitative reaction of the 4-thiouridine residue at position 8 in the tRNA^{Arg}I to cytidine-13, assayed by borohydride reduction as described by Ofengand *et al.*, 1974) or treated with iodoacetamide (which specifically blocks the thiocytidine residue; Kruse *et al.*, 1978) prior to BAPTD treatment (see text).

Binding of derivatized tRNA^{Arg}I to the ribosomal A, P or E sites

mRNA analogues (Figure 1) were prepared from DNA templates by T7 transcription, as described by Stade *et al.* (1989) and Dontsova *et al.* (1992). In the following paragraphs, all incubations were performed at 37°C for the times indicated, and all buffers contained 50 mM HEPES–KOH pH 7.5 and 1 mM 2-mercaptoethanol, together with varying concentrations of NH_4Cl and $MgCl_2$, again as indicated. For the tRNA binding experiments (cf. Rheinberger *et al.*, 1988; Wower *et al.*, 1993), either 70S tight couple ribosomes (250 pmol in 200 μl) or 70S ribosomes reconstituted from 30S and 50S subunits (250 pmol each in 200 μl) were used; in the latter case the subunits were activated for 10 min at 200 mM NH_4^+ and 20 mM Mg^{2+} before adding to the reaction mixtures.

A site binding. 70S tight couples were incubated for 10 min in 60 mM NH_4^+, 7.5 mM Mg^{2+}, with a 4-fold excess of mRNA (see text) and a 2-fold excess of tRNA^{fMet}. Then the Mg^{2+} concentration was raised to 10 mM, an equimolar amount (with respect to 70S ribosomes) of ^{32}P-labelled BAPTD-derivatized Arg-tRNA^{Arg}I was added, and incubation continued for 15 min. In the case of reconstituted 70S ribosomes, the first incubation was made with 30S subunits instead of 70S tight couples, at 10 mM Mg^{2+}; then 50S subunits were added, and the second incubation was carried out as for the tight couples, but at 15 mM Mg^{2+}.

P site binding. 70S tight couples were incubated for 10 min in 60 mM NH_4^+, 7.5 mM Mg^{2+} with a 0.75-fold molar amount of ^{32}P-labelled BAPTD-tRNA^{Arg}I, and with either a 4-fold excess of mRNA (see text) or without mRNA. The Mg^{2+} concentration was then raised to 10 mM and incubation continued for a further 10 min. In the case of reconstituted 70S ribosomes, the first incubation was made with 30S subunits in the absence of mRNA, either as just described, or with 100 mM NH_4^+, 10 mM Mg^{2+}. Then 50S subunits were added, and the second incubation was carried out for 15 min either at 60 mM NH_4^+, 10 mM Mg^{2+} or at 100 mM NH_4^+, 15 mM Mg^{2+}.

E site binding. The P site was first blocked by incubating for 15 min with a 2-fold excess of either tRNA^{Phe} or tRNA^{fMet} in the presence of a 4-fold excess of appropriate mRNA (see text), using either 70S tight couples or 30S subunits in 100 mM NH_4^+, 10 mM Mg^{2+}. 50S subunits were then added (in the case of the reconstituted 70S ribosomes). Next, a 0.5–0.7 molar amount of ^{32}P-labelled BAPTD-tRNA^{Arg}I was added, and incubation continued for 10 min with the Mg^{2+} concentration raised to either 15 or 20 mM.

Cross-linking and analysis of cross-linked products

The tRNA–mRNA–ribosome complexes were irradiated for 10 min at 350 nm, as described by Tate *et al.* (1990), and then applied to a series of sucrose gradients (see text, and Stade *et al.*, 1989) in order to isolate 16S rRNA or 30S ribosomal protein fractions cross-linked to BAPTD-tRNA^{Arg}I. Typical yields of ^{32}P-labelled BAPTD-tRNA^{Arg}I cross-linked to 16S RNA in a 250 pmol experiment were of the order of 20 000–80 000 c.p.m., with the corresponding amounts of radioactivity cross-linked to ribosomal protein being 3- to 4-fold higher. Cross-linked ribosomal proteins were identified by the immobilized agarose–antibody method (Gulle *et al.*, 1988; Rinke-Appel *et al.*, 1991), and cross-link sites on the 16S RNA were determined by treatment with ribonuclease H in the presence of selected pairs of oligodeoxynucleotides (Rinke-Appel *et al.*, 1991) followed by primer extension analysis (Moazed *et al.*, 1986). In order to minimize thermal breakdown of the cross-linked complexes, the ribonuclease H digestions were carried out for 10 min at 55°C (without a pre-incubation step) instead of the usual 30 min, and the primer annealing reaction for the primer extension analysis was made at 55°C instead of 70°C.

Acknowledgements

We are grateful to Dr B.P.Baskunov for recording mass spectra, Dr V.P.Kutyshenko for recording NMR spectra and Dr V.N.Medvedkin for performing C, H, N analyses of the BAPTD. We also thank Dr K.H.Nierhaus for many useful discussions. The work was in part supported by a grant from the Deutsche Forschungsgemeinschaft.

References

Bhangu,R. and Wollenzien,P. (1992) *Biochemistry*, **31**, 5937–5944.
Bochkariov,D. and Kogon,A. (1992) *Anal. Biochem.*, **204**, 90–95.
Brimacombe,R. (1991) *Biochimie*, **73**, 927–936.
Brimacombe,R., Atmadja,J., Stiege,W. and Schüler,D. (1988) *J. Mol. Biol.*, **199**, 115–136.
Brimacombe,R., Mitchell,P., Osswald,M., Stade,K. and Bochkariov,D. (1993a) *FASEB J.*, **7**, 161–167.
Brimacombe,R., Döring,T., Greuer,B., Jünke,N., Mitchell,P., Müller,F., Osswald,M., Rinke-Appel,J. and Stade,K. (1993b) In Nierhaus,K.H., Franceschi,F., Subramanian,A.R., Erdmann,V.A. and Wittmann-Liebold,B. (eds), *The Translational Apparatus*. Plenum Press, New York, pp. 433–444.
Brunner,J. and Semenza,G. (1981) *Biochemistry*, **20**, 7174–7182.
Brunner,J., Senn,H. and Richards,F.M. (1980) *J. Biol. Chem.*, **255**, 3313–3318.
Chen,J.K., Frank,L.A., Hixson,S.S. and Zimmermann,R.A. (1985) *Biochemistry*, **24**, 4777–4784.
Ciesiolka,J., Gornicki,P. and Ofengand,J. (1985) *Biochemistry*, **24**, 4931–4938.
Dolder,M., Michei,H. and Sigrist,H. (1990) *J. Protein Chem.*, **9**, 407–415.
Dontsova,O., Dokudovskaya,S., Kopylov,A., Bogdanov,A., Rinke-Appel,J., Jünke,N. and Brimacombe,R. (1992) *EMBO J.*, **8**, 3105–3116.
Gnirke,A., Geigenmüller,U., Rheinberger,H.J. and Nierhaus,K.H. (1989) *J. Biol. Chem.*, **264**, 7291–7301.
Gulle,H., Hoppe,E., Osswald,M., Greuer,B., Brimacombe,R. and Stöffler,G. (1988) *Nucleic Acids Res.*, **16**, 815–832.
Hixson,S.H. and Hixson,S.S. (1975) *Biochemistry*, **14**, 4251–4254.
Klabunde,K.J. and Burton,D.J. (1970) *J. Org. Chem.*, **35**, 1711–1712.
Kröger,M., Sprinzl,M. and Cramer,F. (1976) *Liebigs Ann. Chem.*, **1976**, 1395–1405.
Kruse,T.A., Clark,B.F.C. and Sprinzl,M. (1978) *Nucleic Acids Res.*, **5**, 879–892.
Mitchell,P., Stade,K., Osswald,M. and Brimacombe,R. (1993) *Nucleic Acids Res.*, **21**, 887–896.
Moazed,D. and Noller,H.F. (1989) *Cell*, **57**, 585–597.
Moazed,D. and Noller,H.F. (1990) *J. Mol. Biol.*, **211**, 135–145.
Moazed,D., Stern,S. and Noller,H.F. (1986) *J. Mol. Biol.*, **187**, 399–416.
Nolan,J.M., Burke,D.H. and Pace,N.R. (1993) *Science*, **261**, 762–765.
Ofengand,J., Delaney,D. and Bierbaum,J. (1974) *Methods Enzymol.*, **29**, 673–684.
Podkowinski,J. and Gornicki,P. (1989) *Nucleic Acids Res.*, **17**, 8767–8782.
Prince,J.B., Taylor,B.H., Thurlow,D.L., Ofengand,J. and Zimmermann,R.A. (1982) *Proc. Natl Acad. Sci. USA*, **79**, 5450–5454.
Rheinberger,H.J., Geigenmüller,U., Wedde,M. and Nierhaus,K.H. (1988) *Methods Enzymol.*, **164**, 658–670.
Rinke-Appel,J., Jünke,N., Stade,K. and Brimacombe,R. (1991) *EMBO J.*, **8**, 2195–2202.
Rinke-Appel,J., Jünke,N., Brimacombe,R., Dokudovskaya,S., Dontsova,O. and Bogdanov,A. (1993) *Nucleic Acids Res.*, **21**, 2853–2859.
Schilling-Bartetzko,S., Franceschi,F., Sternbach,H. and Nierhaus,K.H. (1992) *J. Biol. Chem.*, **267**, 4693–4702.
Sprinzl,M., Hartmann,T., Weber,J., Blank,J. and Zeidler,R. (1989) *Nucleic Acids Res.*, **17**, r1–r172.
Stade,K., Rinke-Appel,J. and Brimacombe,R. (1989) *Nucleic Acids Res.*, **17**, 9889–9908.
Steiner,G., Kuechler,E. and Barta,A. (1988) *EMBO J.*, **7**, 3949–3955.
Stewart,R. and Van der Linden,R. (1960) *Can. J. Chem.*, **38**, 399–406.
Sylvers,L.A., Kopylov,A.M., Wower,J., Hixson,S.S. and Zimmermann,R.A. (1992) *Biochimie*, **74**, 381–389.

Tate,W., Greuer,B. and Brimacombe,R. (1990) *Nucleic Acids Res.*, **18**, 6537–6544.
Wower,J., Hixson,S.S. and Zimmermann,R.A. (1989) *Proc. Natl Acad. Sci. USA*, **86**, 5232–5236.
Wower,J., Malloy,T.A., Hixson,S.S. and Zimmermann,R.A. (1990) *Biochim. Biophys. Acta*, **1050**, 38–44.
Wower,J., Sylvers,L.A., Rosen,K.V., Hixson,S.S. and Zimmermann,R.A. (1993a) In Nierhaus,K.H., Franceschi,F., Subramanian,A.R., Erdmann,V.A. and Wittmann-Liebold,B. (eds), *The Translational Apparatus*. Plenum Press, New York, pp. 455–464.
Wower,J., Scheffer,P., Sylvers,L.A., Wintermeyer,W. and Zimmermann,R.A. (1993b) *EMBO J.*, **12**, 617–623.

Received on February 3, 1994